Status and plans for the CMS High Granularity Calorimeter upgrade project

Eva Sicking (CERN)
on behalf of the CMS collaboration

12th International Conference on Position Sensitive Detectors
September 15, 2021

LHC and HL-LHC timeline

Experimental conditions from LHC to High-Luminosity-LHC:

Luminosity:	$2\times10^{34}\,s^{-1}cm^{-2}$	$\rightarrow$	$5–7.5\times10^{34}\,s^{-1}cm^{-2}$
Radiation background:	10^{14} neq/cm^2	$\rightarrow$	$1–1.5\times10^{16}$ neq/cm^2
Pile-up events:	O(40)	$\rightarrow$	O(140–200)

LHC and HL-LHC timeline

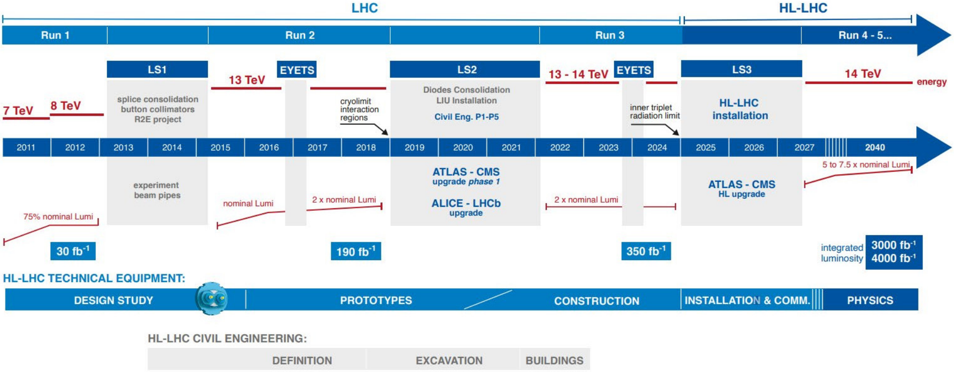

Detector adaptations from LHC to High-Luminosity-LHC:

Luminosity:	improved trigger and computing
Radiation background:	radiation-tolerant sensors and electronics
Pile-up events:	precise timing and increased granularity

CMS upgrade for HL-LHC

Tracker:
Radiation tolerant, high granularity, less material, tracks in hardware trigger (L1), coverage up to $|\eta| = 3.8$

Barrel Calorimeter:
New BE/FE electronics, ECAL: lower temp., HCAL: partially new scintillator

Timing layer:
MIP timing to $30 - 60$ ps, coverage up to $|\eta| = 3.0$

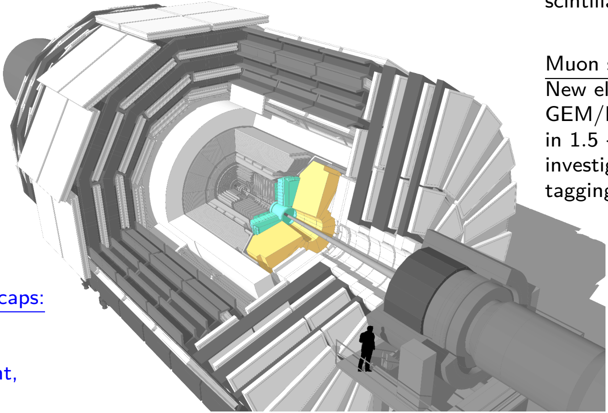

Muon system:
New electronics GEM/RPC coverage in $1.5 < |\eta| < 2.4$, investigate Muon tagging at higher η

Calorimeter endcaps:
Coverage $1.5 < |\eta| < 3.0$, radiation tolerant, high granularity, precise hit/cluster timing

CMS CE a.k.a. HGCAL

Calorimeter Endcap or
High Granularity CALorimeter

- $1.5 < \eta < 3.0$
- 215 tons per endcap
- Full system at -35°C
- ~620 m² of silicon sensors,
  ~6M channels in
  ~30k modules,
  cell size 0.5–1.1 cm²
- ~400 m² of scintillator,
  ~240k tiles + SiPMs in
  ~4000 boards,
  tile size 4–30 cm²
- Power at end of HL-LHC:
  125 kW per endcap

- CALICE-inspired imaging calorimeter optimised for particle flow analysis

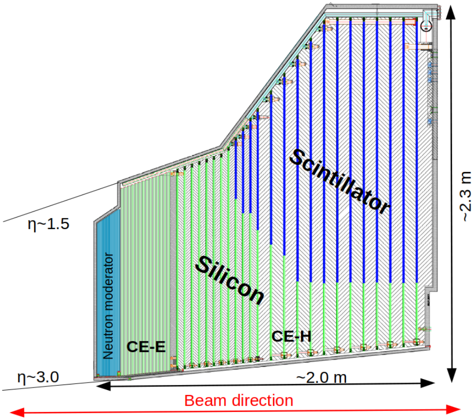

- El.-mag. section **CE-E**: **Si**, Cu, CuW, Pb absorbers, 28 layers, $25X_0$&$\sim 1.3\lambda$
- Hadronic section **CE-H**: **Si+scintillator+SiPM**, steel absorbers, 22 layers, $\sim 8.5\lambda$

▸ HGCAL TDR

620 m^2 of silicon sensors

8-inch Low-Density sensor

$\sim$ 200 cells of 1.1 cm^2 size

300 µm & 200 µm active thickness

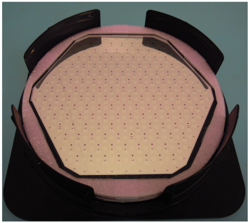

8-inch High-Density sensor

$\sim$ 450 cells of 0.5 cm^2 size

120 µm active thickness

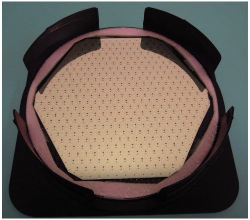

- Used for CE-E and high-radiation regions in CE-H
  - Thickness and granularity adapted to radiation field (→backup)
- Hexagonal silicon sensor geometry
  - Largest tile-able polygon
  - Maximise wafer usage and aid tiling
  - "Partial" sensors to tile border regions (→backup)
- 8-inch wafers
  - Reduces number of modules w.r.t. 6-inch wafers
  - New production process and radiation-hardness qualification
- Planar, DC-coupled, p-type sensor pads
  - p-type more radiation tolerant than n-type sensors
- Sensor producer HPK

Details of prototype sensor layout

Standard & calibration cells

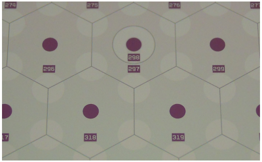

Enlarged guard ring contact

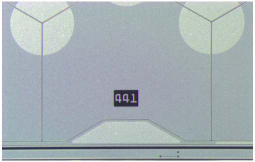

Silicon radiation-hardness qualification

Full 8-inch sensors

- Neutron irradiation of 8-inch wafers up to $1 \cdot 10^{16}$ neq/cm^2 at Rhode Island Nuclear Science Centre, US
- In 2020/2021 irradiated 40 HPK prototype sensors $\rightarrow$ Goal: identify best production process

RINSC 8-inch irradiation slot

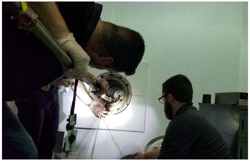

Probe card system for full-wafer IV+CV tests

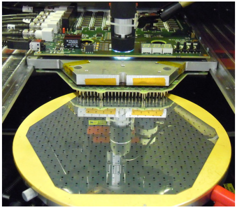

Per-cell leakage current at $1 \cdot 10^{16}$ neq/cm^2

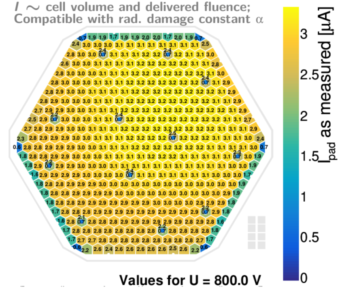

IV curves for 4 production process variants

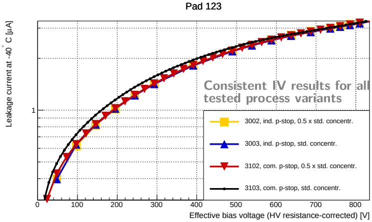

Silicon modules

8-inch prototype module stack-up

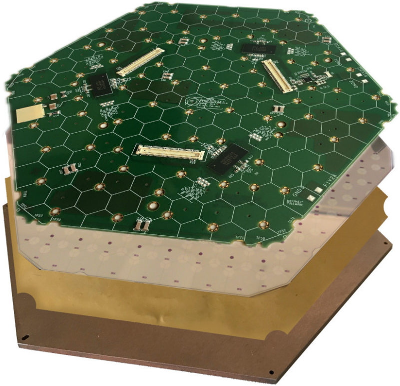

Wirebonds to cells, GR, bias voltage contact

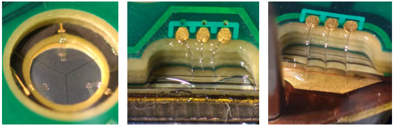

- Glued sandwich of PCB, Si sensor, biasing/insulation layer and baseplate (rigidity, cooling, absorber element)
- Wire-bonding from PCB to silicon

Module assembly on automated Gantries

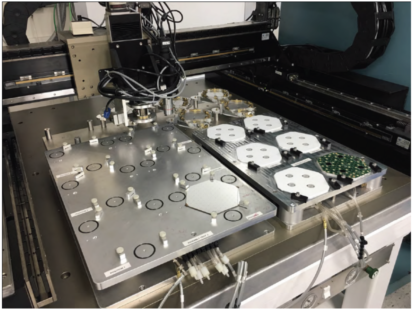

- Successfully operated O(100) 6-inch module prototypes in beam tests
- This week, beam test at CERN with 8-inch module prototypes

400 m^2 of scintillator for low-rad. regions

CALICE AHCAL SiPM-on-tile prototype

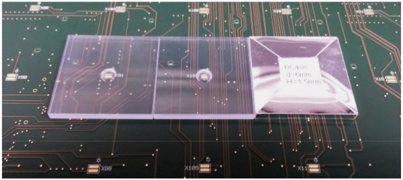

$S/N > 5$ after $3\,ab^{-1}$

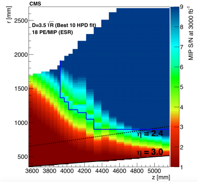

Injection molded tile

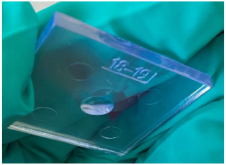

Tile wrapping machine

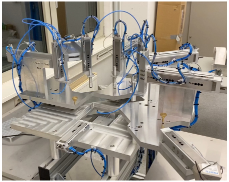

Tileboard prototype with irradiated SiPMs

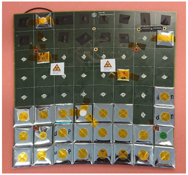

- Cheaper than silicon → use in low radiation regions where $S/N > 5$ can be maintained up to $3\,\text{ab}^{-1}$
- 240k SiPMs integrated into the PCB, cooled operation to mitigate increasing leakage current
- Prototypes of injection-molded tiles and cast and machined tiles
- Development of automated wrapping and automated assembly of tile-module
- Successfully operated tileboards in beam tests, including also irradiated SiPMs

Passive absorber plates and services

CE-H steel absorber plates

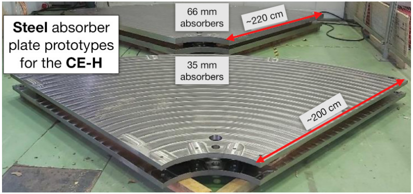

HGCAL detector services mockup

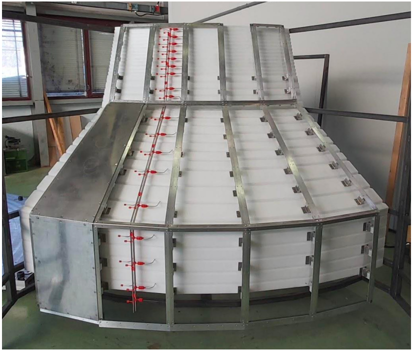

CE-E lead sandwich absorber plate prototype

- Procurement process of 600 tons of stainless steel started
- Stringent limits on relative magnetic permeability
- Achieved 1 mm flatness for CE-H steel absorber plates
- CE-E lead sandwich absorber development challenging due to relative softness and lower workability
- Mock-up structures to study installation steps and on-detector services locations

Front end electronics: Challenges

- Low noise (<2500e) and high dynamic range (0.2 fC –10 pC)
- Timing information to O(10 ps)
- Radiation tolerant
- < 20 mW per channel (cooling limitation)
- Height limitation of layers hosting ASICs

V3 HGCROC ASIC
both for silicon and scint. modules

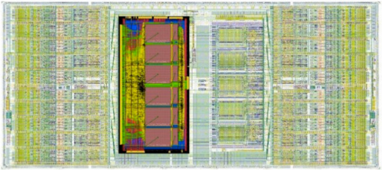

ECON concentrator ASIC

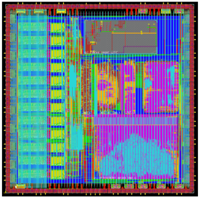

Cassette mockup

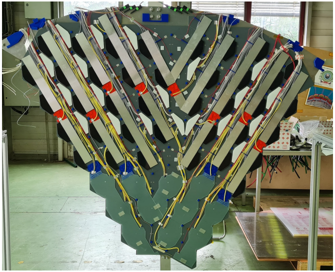

- ECON-T: aggregation and compression of cell sums for L1 trigger
- ECON-D: common-mode estimation and zero-suppression of triggered data

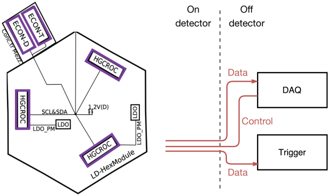

Offline reconstruction

Simulation of 140 pileup events in CMS

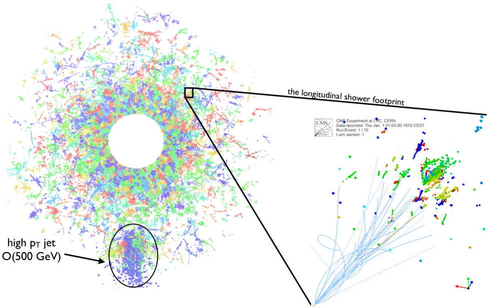

TICL approach

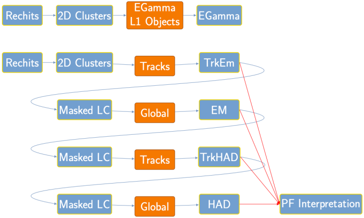

- Explore multiple reconstruction concepts: iterative reconstruction based on tracker reconstruction (TICL) as well as end-to-end Machine-Learning based approaches (ML4Reco)
- The Iterative CLustering (TICL) workflow
  - 1) merge hits to 2D clusters,
    2) merge clusters to tracks
  - Iterative approach: Reconstruct clearly identifiable objects first, then continue with remaining objects

TICL tracksters:
reconstruction of two close-by photons

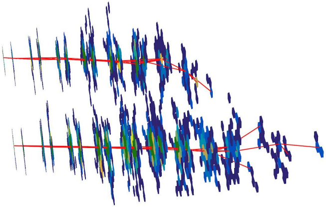

Beam tests in 2016–2018

using 6-inch silicon modules and CALICE Scint. AHCAL

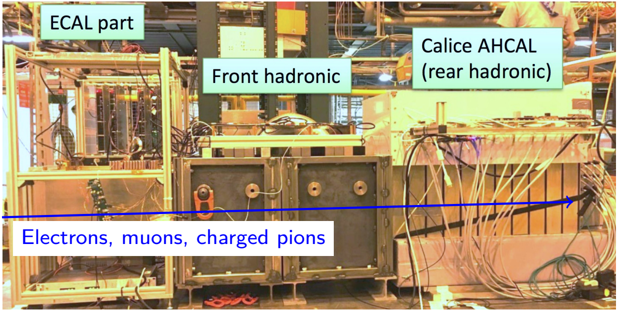

Front hadronic layer

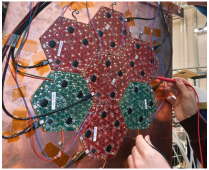

Energy deposits in space full prototype

Publication outlook

- Construction and Commissioning of CMS CE prototype silicon modules ▸ link
- The DAQ System of the 12,000 Channel CMS High Granularity Calorimeter Prototype ▸ link
- El.-mag. response
- Hadronic response
- Precise timing
- SKIROC2-CMS ASIC beam tests

Beam tests in 2016–2018

using 6-inch silicon modules and CALICE Scint. AHCAL

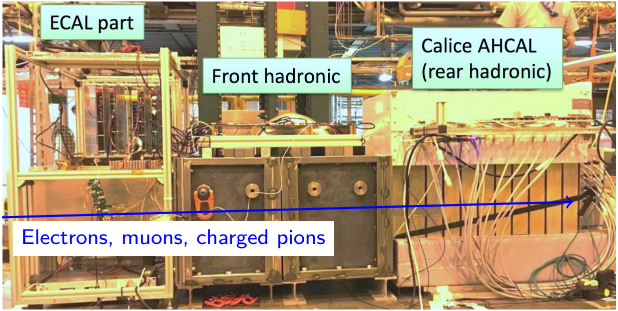

Time of Arrival in ECAL part only
Snapshot of shower development within ∼1 ns (blue=early, yellow=late)

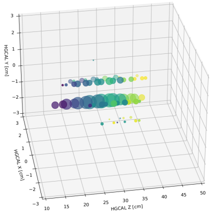

Front hadronic layer

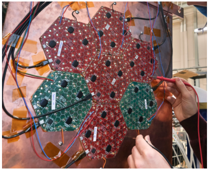

Publication outlook

- Construction and Commissioning of CMS CE prototype silicon modules ▸ link
- The DAQ System of the 12,000 Channel CMS High Granularity Calorimeter Prototype ▸ link
- El.-mag. response
- Hadronic response
- Precise timing
- SKIROC2-CMS ASIC beam tests

Beam test results for el.-mag. showers

Linearity

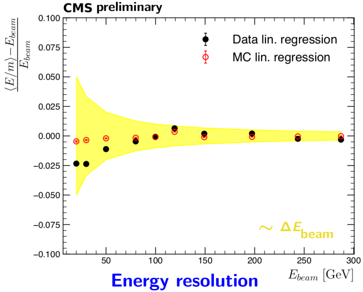

6-inch prototype results

- Linearity better that 3% for data and 1.5% for simulation
- Stochastic term of energy resolution of 21–22$\sqrt{\text{GeV}}$%
- Constant term of 0.6%
- Good agreement between data and simulation, also for position and shower axis resolution

Energy resolution

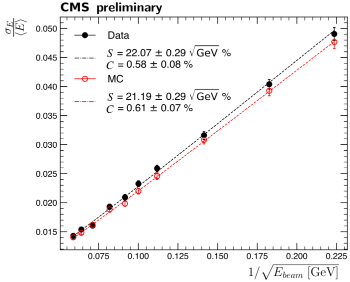

Position resolution in layer 7

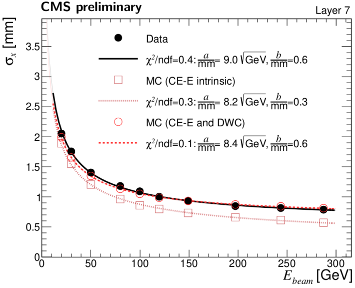

Beam test results for el.-mag. showers

Linearity

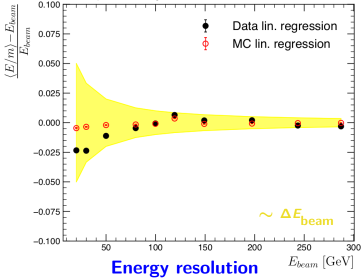

6-inch prototype results

- Linearity better that 3% for data and 1.5% for simulation
- Stochastic term of energy resolution of 21–22$\sqrt{\text{GeV}}$%
- Constant term of 0.6%
- Good agreement between data and simulation, also for position and shower axis resolution

Energy resolution

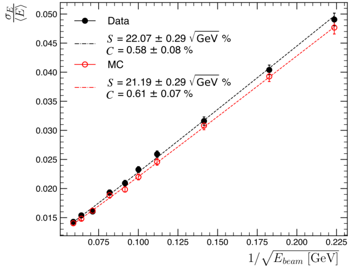

Shower axis pointing resolution

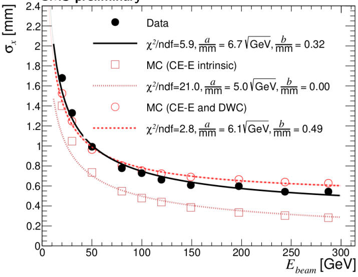

Recent CE re-optimisation

- Prototyping improved understanding of front-end chip size and tolerances of absorber layers
- Adapt geometry to realistic tolerances while preserving overall radiation/interaction lengths
- Example: Number of CE-E layers reduced from 28 to 26 per endcap to minimise overall risk with minimal impact of performance

Impact on energy resolution in CE-E only

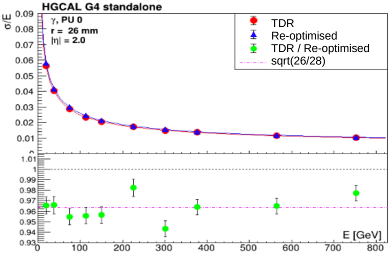

Layer structure of TDR (2018)

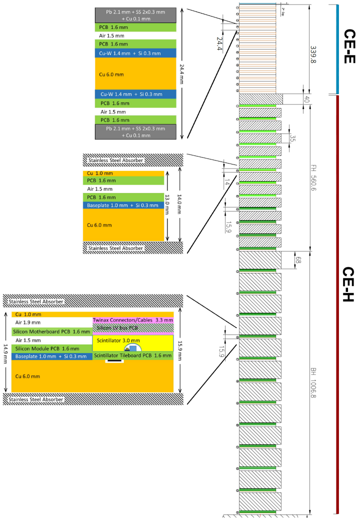

Recent CE re-optimisation

- Prototyping improved understanding of front-end chip size and tolerances of absorber layers
- Adapt geometry to realistic tolerances while preserving overall radiation/interaction lengths
- Example: Number of CE-E layers reduced from 28 to 26 per endcap to minimise overall risk with minimal impact of performance

Impact on energy resolution in CE-E only

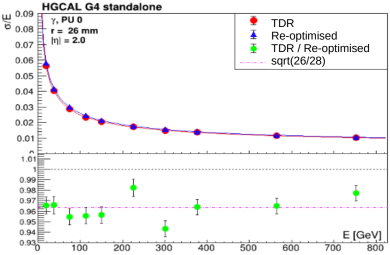

Reoptimisation of CE layer structure

	TDR	Re-optimised
# layers in CE-E, sampling layout	28, uniform	**26; last four thickened**
# layers in CE-H (all Si)	8	**7**
# layers in CE-H (mixed)	14	**14**
CE-H: thickness of thin/ thick absorbers	35.0mm / 66.0 mm	**41.5 mm / 60.7 mm**
Depth of CE-E	25.4 X_0	**27.7 X_0**
Total depth	9.85 λ	**9.97 λ**

Summary and Outlook

- Lots of progress since the Technical Proposal (2015) and the Technical Design Report (2018)
- Several key components approach end of prototyping phase
- Ongoing activity towards Engineering Design Report
  - Finalisation of designs
  - Qualification of final prototypes
  - Assembly of modules with final prototypes in assembly centres and beam tests
  - Market surveys and orders
  - Pre-productions
- Next major steps
  - CE Engineering Design Report in summer 2022
  - CE production start in 2022
  - HL-LHC start in 2027

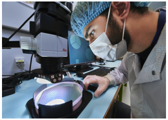

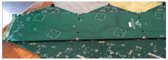
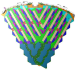
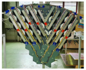
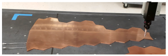
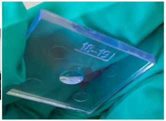
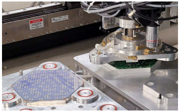
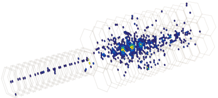
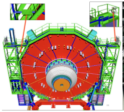


CERN

Backup

Requirements on new calorimeter endcap

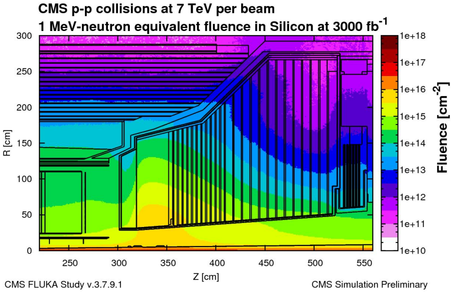

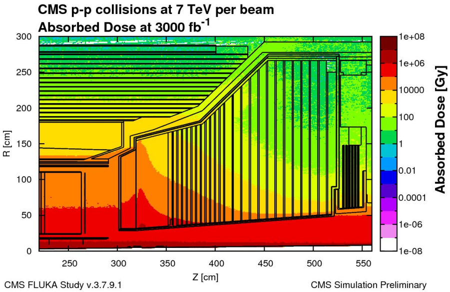

- Radiation hardness
  - Fluences from 1×10^{12} neq/cm^2 to 1×10^{16} neq/cm^2
  - Dose from 10 Gy to 1 MGy
- Spatial and time resolution
  - Resolve energy deposits originating from pile-up vertices spread over O(10 cm) and O(100 ps)

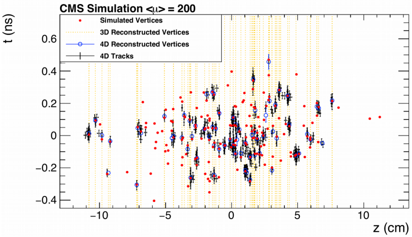

Silicon radiation-hardness qualification

Test structures in neutron and X-ray irradiation

Charge collection eff. vs. fluence

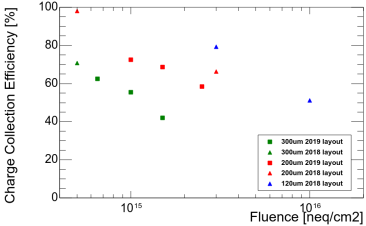

Leakage current vs. fluence

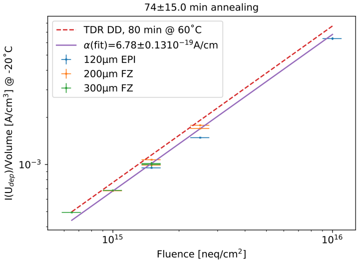

- Optimise sensor thickness to fluence
  - Thin sensors for high fluence regions
  - Lower starting signal before irradiation maintained to higher fluences
- Adapt operation to rad. environment
  - Increase bias voltage up to 800 V to compensate signal loss
  - Operation at −35°C to reduce radiation-induced leakage current
- Identify best HPK oxide variant using X-ray irradiations

Oxide charge density vs. dose

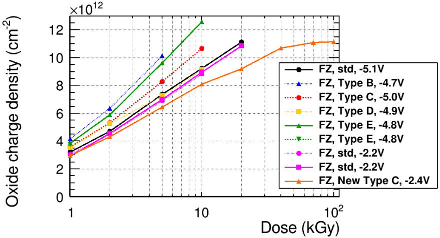

Silicon cassettes

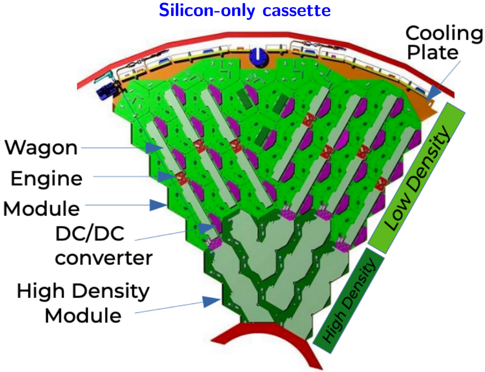

- Modules are combined to cassettes
- Self-supporting sandwich structures (with absorbers)
- Modules placed on both sides of Cu cooling plate and closed with Pb plates

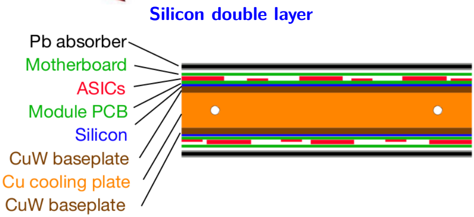

Layer structure

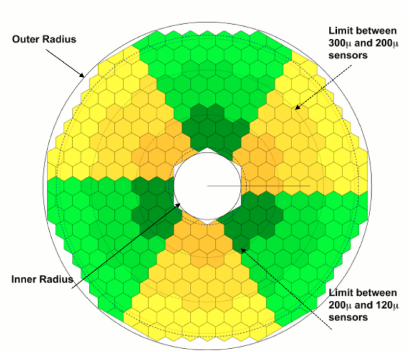

- Silicon-only layer (in CE-E) indicating cassettes (green and yellow) and different sensor thicknesses (shades)

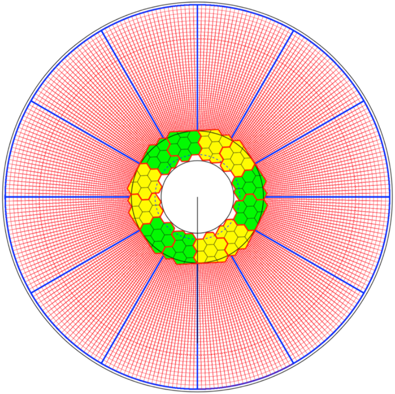

- Mixed layer (in CE-H) with silicon at high η and scintillator+SiPM at low η

Multi-Geometry wafers

Low Density Multi-Geometry Wafer

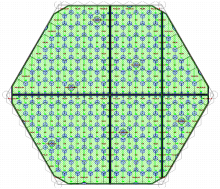

High Density Multi-Geometry Wafer

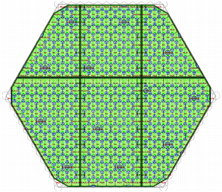

LD partial sensor layout names

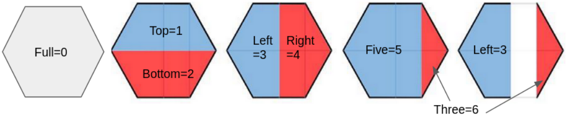

HD partial sensor layout names

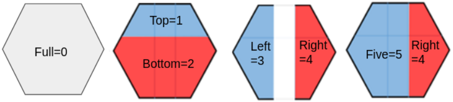

- Border regions of endcap will be tiled with partial sensors made from multi-geometry wafers
- Partial sensors allow increase in coverage of the detector
- Partials sensors increase complexity of the detector design significantly (increase in number of sensor variants, module PCBs, assembly tools, ...)